Greek Letters

α_0 = defined in Eq. 13
α_1 = defined in Eq. 14
β = kinetic constant (K/C_{Ao}^2)
γ = kinetic constant (K/C_{Ao})
ϵ = nondimensional deactivation rate constant $(k_d C_{Ao}^n/k)$

LITERATURE CITED

Chu, C., "Effect of Adsorption on the Fouling of Catalyst Pellets," *Ind. Eng. Chem. Fundamentals*, 7, 509 (1968).

Cole, J. D., *Perturbation Methods in Applied Mathematics*, Blaisdell, Waltham, Mass. (1968).

De Vera, A. L., and A. Varma, "Substrate-Inhibited Enzyme Reaction in a Tubular Reactor with Axial Dispersion," *Chem. Eng. Sci.*, 34, 275 (1979).

Do, D. D., and R. H. Weiland, "Catalyst Deactivation in an Isothermal CSTR with First-Order Chemical Kinetics," *Chem. Eng. J.*, (1979a).

Do, D. D., and R. H. Weiland, "Catalyst Deactivation in an Isothermal CSTR with N-th Order and Michaelis-Menten Kinetics," *Chem. Eng. J.*, (1979b).

Do, D. D., and R. H. Weiland, "Consistency between Rate Expressions for Enzyme Reactions and Deactivation," *Biotech. Bioeng.*, **22**, 1087 (1980c).

Ho, T. C., "Uniqueness Criteria of the Steady State in Automotive Catalysis," *Chem. Eng. Sci.*, 31, 235 (1976).

Kam, E. K. T., and R. Hughes, "Nonisothermal Fouling of Catalyst Pellets Using Langmuir-Hinshelwood Fouling Kinetics," *AIChE J.*, **25**, 359 (1979).

Laidler, K., and P. S. Bunting, *The Chemical Kinetics of Enzyme Action*, 2nd ed., Oxford University Press, Oxford, England (1973).

Lin, S. H., "An Analysis of Immobilized Enzymatic Reaction in a Packed-bed Reactor with Enzyme Denaturation," *Chem. Eng. J.*, 14, 129 (1977).

Nayfeh, A. H., *Perturbation Methods*, Wiley-Interscience, New York (1973).

Pereira, C. J., and A. Varma, "Uniqueness Criteria of the Steady State in Automotive Catalysis," *Chem. Eng. Sci.*, 33, 1645 (1978).

Manuscript received October 1, 1979; revision received April 28, and accepted May 1, 1980.

Determination of Interaction Second Virial Coefficients; He-CO_2 System

J. C. HOLSTE,
M. Q. WATSON,
M. T. BELLOMY,
P. T. EUBANK,
and
K. R. HALL

Chemical Engineering Department
Texas A&M University
College Station, TX 77843

We have obtained values for interaction second virial coefficients of the helium-carbon dioxide system in the range $230 \leq T/K \leq 300$. Our experimental technique is essentially the Burnett mixing method described by Hall and Eubank (1973, 1974). We have modified the analysis to account for higher-order effects and to detect significant systematic errors. We also report virial coefficients for the pure components: helium in the range $100 \leq T/K \leq 300$ and carbon dioxide at 300 K.

SCOPE

Interaction second virial coefficients, B_{ij}, contain information about mixtures which is essential for both theoretical and practical applications. Within statistical mechanics, B_{ij} reflects molecular interactions between unlike molecules and provides insight for theoretical mixture models. On the practical side, B_{ij} is necessary for thermodynamic calculations at low pressure when the application dictates use of the (truncated) virial equation.

The normal method for obtaining B_{ij} is reduction of mixture second virial coefficients, B_m. This is the most obvious but least accurate method. The sources of inaccuracies are experimental errors in the B_{ii} and B_m as well as any errors in composition determination. Edwards and Roseveare (1942) appear to have pioneered this method. Knobler et al. (1959) developed a significantly better technique: the differential pressure method. Their technique eliminated composition and B_m as experimental parameters but retained the B_{ii} explicitly and ignored corrections for the effects of higher-order terms in the virial equation. Although other procedures are possible for obtaining B_{ij} (reduction of vapor-liquid equilibrium data; analysis of chromatographic data), these two techniques have produced the bulk of the B_{ij} data and essentially all of the precise values.

In this project, we extend a technique for isothermal determination of B_{ij} originally proposed by Hall and Eubank (1973). Their method was "direct" in that the pure-component virial coefficients, B_{ii}, did not appear explicitly. Because B_{ii} was a principal source of error in previous methods for obtaining B_{ij}, the direct method appeared to have potentially greater accuracy. We chose to evaluate the method with mixtures of simple molecules, because they are more tractable for theoretical studies. This particular test involves helium (a spherical, nonpolar molecule) and carbon dioxide (a linear, quadrupolar molecule).

Correspondence concerning this paper should be addressed to K. R. Hall.

0001-1541-80-3374-0954-$01.25.

CONCLUSIONS AND SIGNIFICANCE

The B_{ij} values we have determined are for the helium-carbon dioxide system at 10 K intervals from 230 to 300 K. These results indicate that the method proposed by Hall and Eubank (1973) is a definite improvement over earlier techniques for determining B_{ij} data.

In the process of applying the direct method, we have developed procedures for including and minimizing the effects of higher order terms in the virial equation (not considered in the original article). We also carefully studied possible systematic errors in the experiment, and it appears that our experimental accuracy is approximately equal to our experimental precision.

Because we are able to collect accurate data relatively quickly, we shall embark on a program to produce B_{ij} for several systems of interest to both theoreticians and practicing engineers. These systems will involve both natural and synthetic gas components. We expect that the long-range value of the data will be to provide insight for theoretical mixture models. The immediate value will be for design calculations in the gas processing industry.

Introduction

In many applications, both theoretical and practical, the virial equation is the preferred equation of state for fluids and fluid mixtures. In theoretical studies, this equation is essential because of its precise basis in statistical mechanics. For practical applications, corresponding-states estimates of the virial coefficients may be the only source of information for some fluids.

A statistical-mechanical derivation produces the virial equation in two equivalent forms:

$$Z - 1 = \sum_{k=2}^{\infty} \beta_k \rho^{k-1} = \sum_{k=2}^{\infty} \beta'_k P^{k-1} \tag{1}$$

where Z is the compressibility factor, ρ is the density, P is the pressure and β_k are the virial coefficients. In addition, for mixtures the virial coefficients become:

$$\beta_{2m} \equiv B_m = \sum_i \sum_j y_i y_j B_{ij} \tag{2}$$

$$\beta_{3m} \equiv C_m = \sum_i \sum_j \sum_k y_i y_j y_k C_{ijk} \tag{3}$$

where y_k is the mole fraction of the component. Higher virial coefficients have equivalent sums. Obviously, the fundamental information concerning mixtures resides in the interaction virial coefficients; B_{ij}, C_{ijk}, etc.; not in the mixture virial coefficients; B_m, C_m, etc. The principal goal of this project is to provide values for the interaction second virial coefficient, B_{ij}.

For the current study, we have chosen the helium-carbon dioxide system. Although this system is of limited practical interest, the interaction of a spherical, nonpolar molecule with a linear, quadrupolar molecule is of theoretical significance. For this study, the mixture dew point establishes the minimum temperature, while apparatus design fixes the maximum temperature.

Review of Previous Work

Helium and carbon dioxide are among the most thoroughly studied substances. For example, Kuenen (1895) measured *$P\rho T$* properties for helium before the turn of the century, and helium data still appear in the current literature, although, as in this case, they are usually ancillary data. Cook (1961) and Barieau (1968) have published reviews of thermodynamic properties for helium, and the International Union of Pure and Applied Chemistry (I.U.P.A.C.) has published a volume of thermodynamic tables for helium (Angus et al., 1975). Carbon dioxide is receiving increased attention at this time, primarily because of its significant role in tertiary oil recovery processes. Two collections of CO_2 data are available as monographs: Vukalovich and Altunin (1969) and the I.U.P.A.C. volume by Angus et al. (1973). The book of Dymond and Smith (1969) is a good source of virial-coefficient data for both He and CO_2.

Values of the interaction second virial coefficient have come primarily from determination of mixture second virial coefficients. For a binary mixture, Eq. 2 becomes:

$$B_{12} = (B_m - y_1^2 B_{11} - y_2^2 B_{22})/2y_1 y_2 \tag{4}$$

Edwards and Roseveare (1942) appear to have pioneered use of this model. In their method, the error in B_{12} will be essentially the sum of the errors in the determinations of the compositions, the mixture virial, and the pure fluid virial coefficients. The result is roughly four to five times the error in a pure-fluid virial determination. Knobler et al. (1959) determined B_{12} by observing the pressure change on mixing of two pure fluids originally contained in two identical volumes at the same pressure. The interaction second virial coefficient is related to the relative pressure change on mixing by:

$$B_{12} = \frac{1}{2}(B_{11} + B_{22}) + \frac{2(1 + B_{11}\rho_1)}{\rho_2}\frac{\Delta P}{P} \tag{5}$$

In Eq. 5, the error caused by uncertainties in composition is reduced significantly, but many cases require corrections for third-virial contributions. Hall and Eubank (1973) proposed a new technique using a Burnett cell to determine B_{12}—this is the basic technique used in this work although we have extended it to account for higher-virial effects. It also is a difference technique as will become obvious.

The He-CO_2 interaction virial coefficient has received some attention in the past. The sources we were able to identify include: Pfefferle et al. (1955), Cottrell and Hamilton (1956), Harper and Miller (1957), Brewer (1967), Weems and Miller (1969), Weems and Howard (1970), Linshits et al. (1975), Bellomy (1976), and Pak and Schultz (1978). All authors used the reduction of B_m as in Eq. 4 except Brewer (1967), who used the differential-pressure method, and Bellomy (1976) who used the Hall-Eubank method.

Apparatus

We used a conventional Burnett apparatus in this work. Bellomy (1976), Watson (1978) and Young (1978) present the details of the apparatus which we now summarize. Figure 1 shows the general layout of the apparatus. The sample fluid is entirely within the temperature bath and the pressure is compared to an external pressure medium (helium) by a differential pressure indicator (DPI). The gas-lubricated dead weight gauge (0.1 to 5 MPa) and the mercury manometer (0 to 0.2 MPa) are consistent within 0.01% in the region of overlap (0.1 to 0.2, MPa). The pressure-measurement technique represents a significant advance, and it is described in detail by Holste et al. (1977). We can obtain precisions in pressure measurements of approximately 0.001% and absolute accuracies of approximately 0.015% with this technique, except at the lowest pressures. For the

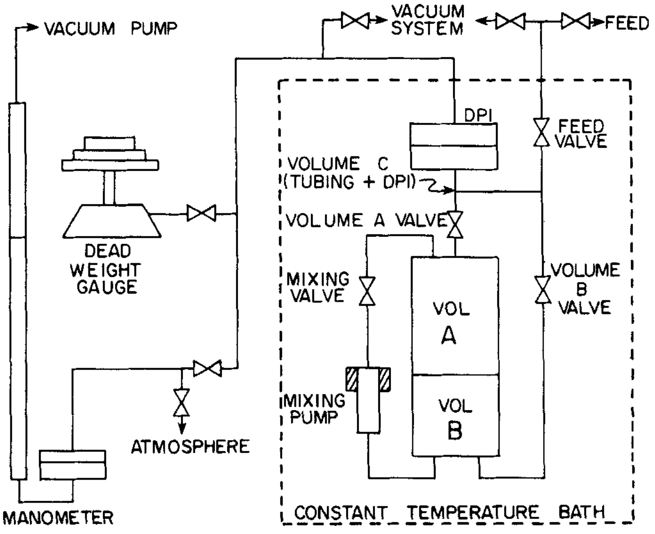

Figure 1. Overall schematic of apparatus.

particular experiments of interest here, extreme precision is of greater importance than absolute accuracy.

Figure 2 shows details of the cryostat schematically. The sample cells are Invar because this alloy has a relatively small coefficient of thermal expansion. (Invar does, of course, limit the use of this apparatus to noncorrosive fluids). Helium gas is the fluid medium in the bath with several advantages: convenience, low cost, high thermal conductivity, extreme temperature capabilities, nontoxic, and nonexplosive. Our platinum resistance thermometer is in the gas stream, and a thermopile provides a measure of thermal gradients in the system. The platinum resistance thermometer temperature is controlled to 0.001 K, and the thermopile indicates gradients of the same magnitude at 300 K (the temperature where all expansions and manipulations occur), while at lower temperatures the gradients are larger, but never exceeding 0.015 K. The mixing pump is similar to the one described by Mansoorian (1975), and it provides mechanical mixing of the sample fluids.

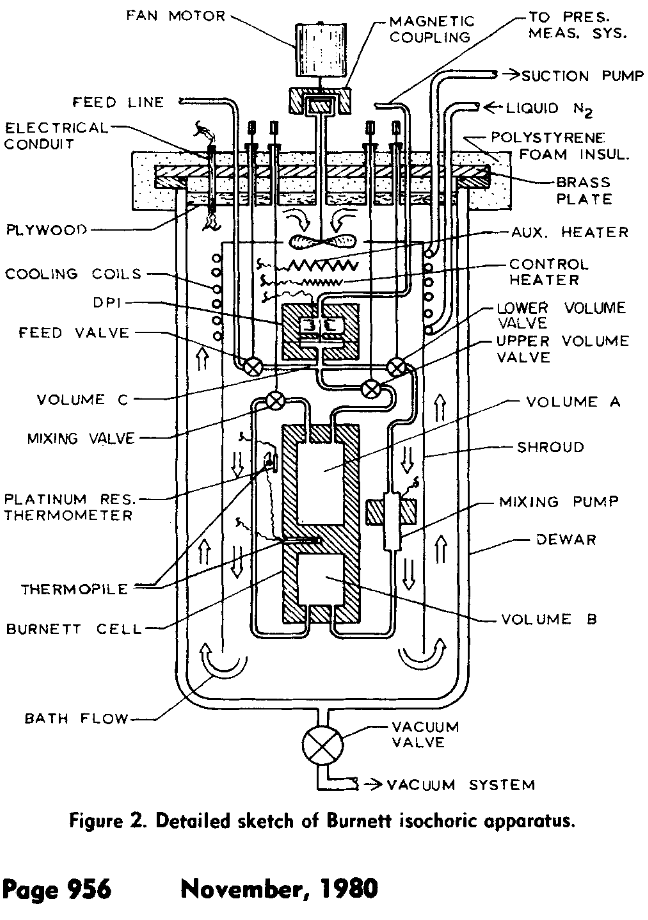

Figure 2. Detailed sketch of Burnett isochoric apparatus.

We used the plumbing arrangement in Figure 3a for this work, but an alternative plumbing scheme (Figure 3b) deserves attention. Note that in this schematic, the valve arrangement allows the feature that no stem packings are included in the combination of volume A and the DPI. This is a particular advantage for isochoric runs (discussed later), particularly when the sample fluid is highly corrosive or strongly adsorbing. The principal disadvantages of this arrangement are that volume A must be filled to fill volume B to a known pressure, and the DPI null reading can be determined only at the end of the entire run. For the arrangement in 3a, each volume can be filled independently and the null can be verified after every expansion, but one valve stem must remain in the principal experimental volume (A + DPI).

Burnett Analysis

A conventional Burnett apparatus consists, in principle, of two cells with unspecified volumes connected by a valve. The first cell is filled with the fluid of interest, a series of isothermal expansions into the second volume (evacuated) is performed, and the pressure is measured after each expansion. The continuous series of isothermal expansions constitutes a run, and a run terminates upon reaching the minimum observable pressure. Burnett (1936) conceived the experiment and provided the original analysis. The Burnett relations are well known, but we present special forms that prove advantageous in the statistical analysis of the data.

Because there are seven possible permutations of the Burnett experiment in the apparatus shown in Figure 1, we shall present the analysis in a general form. We also consider both the pressure and density forms of the virial equation for reasons that will become apparent later.

The equation of state for the fluid after the jth expansion is:

$$P_j = \rho_j Z_j RT \tag{6}$$

where T is the temperature and R is the gas constant. (Note that $j = 0$ denotes the original filling.) Because the number of moles is conserved during an expansion, the ratio of the densities before and after the expansion is inversely proportional to the volume available to the fluid. We denote this ratio by N_j and note that:

$$N_j = \rho_{j-1}/\rho_j = V_j'/V_j \tag{7}$$

where V_j is the volume occupied by the fluid before the expansion and V_j' is the volume after the expansion. The cell volumes will distort with pressure, and we define the cell constant relative to the zero pressure value as:

$$N_j = N\frac{(1 + \gamma' P_j)}{(1 + \gamma P_{j-1})} \tag{8}$$

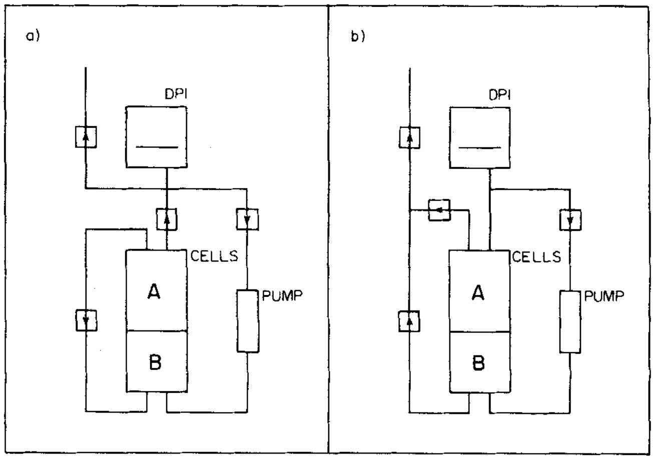

Figure 3. Schematic of tubing arrangement: a) as used for this work; b) suggested by Glowka (arrows point toward valve stem seals).

where N is the undistorted volume ratio while γ and γ' are the pressure distortion coefficients for V and V' respectively. (For high pressure work, higher order pressure coefficients also may be necessary.)

We developed two alternative working equations for data analysis: a pressure-explicit form and a density-explicit form. These forms are respectively:

$$\frac{P_j}{P_{j-1}} = \frac{Z_j}{N_j Z_{j-1}} = \frac{Z_j}{N Z_{j-1}} \left[\frac{1 + \gamma P_{j-1}}{1 + \gamma' P_j}\right]$$

$$= \frac{1}{N} \left[\frac{1 + \gamma P_{j-1}}{1 + \gamma' P_j}\right] \left[\frac{1 + \sum_{k=2}^{\infty} \beta'_k P_j^{k-1}}{1 + \sum_{k=2}^{\infty} \beta'_k P_{j-1}^{k-1}}\right] \tag{9}$$

$$P_j = RT \sum_{k=1}^{\infty} \beta_k \left[\rho_{\min} N^{m-j} \prod_{i=j+1}^{m} \left(\frac{1 + \gamma' P_i}{1 + \gamma P_{i-1}}\right)\right]^{k-1} \tag{10}$$

Eq. 9 is simply a ratio form of Eq. 6 and has adjustable parameters N and β'_k. Eq. 10 results from substituting Eq. 7 written for *m continuous* expansions,

$$\rho_j = \rho_{\min} N_j^{m-j} = \rho_{\min} N^{m-j} \prod_{i=j+1}^{m} \left(\frac{1 + \gamma' P_i}{1 + \gamma P_{i-1}}\right) \tag{11}$$

into the virial equation,

$$P_j = RT \sum_{k=1}^{\infty} \beta_k \rho_j^k \tag{12}$$

and it has adjustable parameters N, $\rho_{\min}$ and β_k. For both Eqs. 9 and 10, we require *a priori* estimates of γ and γ'. The initial guesses of parameters for nonlinear fitting routines with Eqs. 9 and 10 are: $N = P_{m-1}/P_m$, $\rho_{\min} = P_m/RT$ and $\beta_k = \beta'_k = 0$ for all $k \neq 1$.

In both the density and pressure virial cases, an appropriate truncation of the virial equation is necessary. Hall and Canfield (1967), Hall and Righter (1975), and Lee et al. (1978) discussed this problem in depth, and we shall not comment further here. The actual parameter estimates were obtained using an adaptation of the maximum likelihood principle described by Britt and Luecke (1973), and Waxman and Hastings (1971).

Burnett-Isochoric Coupling

The isochoric method is another high-precision technique for collecting $P\rho T$ data. Basically, this method consists of introducing a known mass of sample into a known (calibrated) volume and measuring pressures at a sequence of temperatures. Representative studies using this technique include Weber (1968) and Vennix (1965). A Burnett apparatus can serve equally well as an isochoric apparatus, and Burnett (1963) suggested combining the two experiments into the Burnett-coupled isochoric experiment.

Burnett's coupling procedure is to fill one volume of a Burnett apparatus with a sample to some pressure at a convenient base temperature. Then, varying the temperature and observing pressures produces an isochore. Having adequately traced an isochore, returning to the base isotherm provides an apparatus check for leaks or chemical reactions—the pressure must again be the original pressure. At this point, performing a Burnett expansion establishes a new isochore. Repeating this procedure to the pressure limits of the apparatus constitutes a coupled run; see Hall and Eubank (1972) for details. Figure 4 illustrates the coupled run; the closed squares represent the base isotherm (the Burnett run) and the open circles represent the isochoric trace. Note that all measurements at $T \neq T_b$ occur only in $V_A + V_c$ (Figure 3a) or V_A (Figure 3b). The Burnett-coupled isochoric experiment is a single Burnett isotherm coupling many isochoric runs.

Pope et al. (1972) suggested a different coupling procedure: the isochorically coupled Burnett experiment. This experiment consists of Burnett runs coupled by a few isochoric runs. Each procedure has advantages; we have chosen the Burnett-coupled isochoric experiment for this study. One important feature of the coupled experiment is that every isotherm is a true Burnett run although expansions occur only at the base temperature. Burnett (1963) stated this fact and Pope et al. (1972) presented a proof.

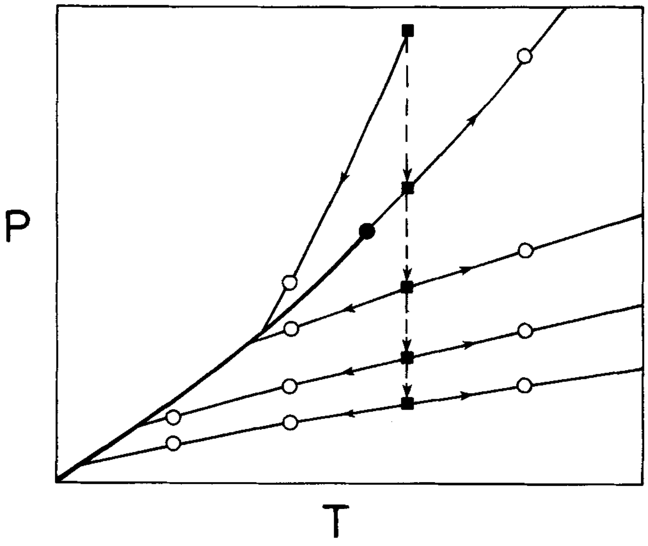

Figure 4. Trace of a Burnett-isochoric run: heavy line ending at critical point (closed circle), vapor pressure curve; open circles and solid squares, experimental measurements; dashed lines, isothermal (Burnett) expansions; and solid lines connecting data, isochores.

The primary advantages of Burnett-isochoric coupling are: generating the $P\rho T$ surface over the entire fluid region with a single sample which minimizes the possibility of sample contamination and the sample cost; operating valves a minimum number of times and at a convenient temperature which reduces the probability of equipment failure or operator error. Other advantages are: linearization of the Burnett analysis in some cases; reduction and possible alleviation of adsorption errors; internal leak tests; precision checks on the pressure measurements; experimental determination of the temperature dependence of the volume distortions. Of course, the Burnett advantage remains: volume and mass need not be measured. The principal disadvantages are: increased run times for a given sample and correlation of experimental errors throughout $P\rho T$ surface. The overall advantages far outweigh the disadvantages. Additional isothermal Burnett runs at the base isotherm further enhance the quality of the data for the entire $P\rho T$ surface.

Burnett Mixing Experiment

Hall and Eubank (1973, 1974) described a Burnett mixing experiment which utilizes conventional Burnett-type measurements to determine mixture properties such as composition, excess volumes, and interaction second virial coefficients. In this isothermal experiment, one volume is filled with a pure fluid to a measured pressure, P_1, and a second volume is filled with a second pure fluid to a pressure, P_2. The fluids then are mixed thoroughly, and the equilibrium pressure of the mixture, P_m, is determined. These data and some previously determined pure-fluid properties and apparatus constants provide the properties of interest.

It is obvious from Figure 3 that there are many possible permutations in the actual performance of this experiment. We develop here a model that is more general in application than that originally presented by Hall and Eubank. We also include third-virial effects in our analysis and utilize extrapolation to zero density to minimize these effects on our B_{ij} values.

Expressions for B_{ij}

We have collected the analysis of the mixing experiment for B_{ij} into Appendix A and present only the results in this section. Experimentally, we shall determine:

$$B_{12}^* = \frac{N_1 N_2 Z_1 Z_2 RT}{2P_1 P_2}\left[P_m - \frac{P_1}{Z_1 N_1^2}(N_1 + Z_1 - 1) - \frac{P_2}{Z_2 N_2^2}(N_2 + Z_2 - 1)\right] \qquad (13)$$

which is equivalent to the expression for B_{ij} presented by Hall and Eubank (1973) but collected in a more general form. Appendix A shows the relationship between B_{ij} and B_{ij}^* as:

$$B_{12}^* = B_{12} + A_1(P_2/Z_2) + A_2(P_2/Z_2)^2 + \ldots \qquad (14)$$

where the A_i are constants for isothermal, constant composition conditions. Clearly, the true value of B_{12} is given by the intercept of a plot of B_{12}^* vs. (P_2/Z_2) for a series of experiments carried out at constant composition. Third-virial contributions introduce slope into the plot; fourth- and higher-order contributions will introduce curvature. The present method, therefore, provides an empirical correction for higher-order effects without explicit knowledge of the actual higher-order virial coefficients. In addition, we shall show later that most significant sources of systematic error in the experiment also introduce curvature to this plot; this provides a further internal consistency test for the experimental data.

Isochoric Extension of Mixing Experiment

The mixing experiment described in the previous section may be combined with the isochoric method using mixtures made at a single temperature to determine interaction second virial coefficients as a function of temperature. In other words, a single set of mixtures, made at a single temperature, is sufficient to evaluate B_{12} values over the entire accessible temperature range. For the isochorically extended experiment, P_1 and P_2 in Eq. 13 come from isochores run for each pure fluid before mixing; P_m comes from an isochore run using the resulting mixture. The analysis of the experiment proceeds as before, except that the fluid densities must be corrected for the temperature expansivity of the cell volume.

Because all isochores are run in the same volume, only a single distortion-correction correlation is required. We define a cell-distortion parameter as:

$$\eta_i = \rho_i^b/\rho_i \qquad (i = 1, 2, m) \qquad (15)$$

where ρ_i is the density at temperature T, ρ_i^b is the density at the mixing temperature T^b, and superscript b denotes properties evaluated at the mixing temperature. The subscript i is necessary because $\eta_i = \eta_i(T, P_i^b)$, *where* P_i^b is the pressure of fluid i at the mixing temperature. The cell-distortion parameters are determined in a self-consistent fashion over the entire pressure and temperature range using pure-helium data. The actual numerical correlation used to describe η_i for our apparatus appears later.

In the analysis of the isochorically extended experiment, the cell-distortion parameters must be included to eliminate algebraically the terms containing the pure-fluid second virial coefficients. The isochoric equivalent of Eq. 13 is:

$$B_{12}^*(T) = \frac{N_1 N_2 Z_1^b Z_2^b R(T^b)^2}{2P_1^b P_2^b T}\left\{\eta_m^2 P_m - \frac{\eta_1^2 P_1}{N_1^2} - \frac{\eta_2^2 P_2}{N_2^2} - \frac{T}{T^b}\left[\frac{P_1^b}{Z_1^b N_1}(\eta_m - \eta_1/N_1) + \frac{P_2^b}{Z_2^b N_2}(\eta_m - \eta_2/N_2)\right]\right\} \qquad (16)$$

We note that for $T = T^b$, $\eta_i = 1$; these equations reduce to their isothermal analogs, as required. In addition, since $\eta_i - 1 \leq 0.001$ in all cases, the temperature dependence of the third-virial contribution (Eq. A12) is principally caused by the temperature dependence of C_{111}, C_{112}, C_{122}, and C_{222}. It is also important to note that the isochoric form of Eq. 14 is:

$$B_{12}^* = B_{12} + A_1(P_2^b/Z_2^b) + A_2(P_2^b/Z_2^b)^2 + \ldots \qquad (17)$$

regardless of temperature.

The advantage of the isochorically extended Burnett mixing experiment becomes apparent upon closer inspection of Eqs. 16 and 17. The only experimental data required at temperatures other than the mixing temperature are P_i and T. To account for second-order effects, the cell-distortion parameter must be known from a previous experiment covering the entire temperature range. Explicit information about pure-fluid compressibility factors and apparatus constants is required only at the mixing temperature. As a result, the mixing temperature may be the most convenient temperature in the range, taking into account such factors as temperature control, adsorption effects, and experimental manipulations. The significant reduction in the total number of required mixtures allows greater care in the preparation of each individual mixture, thereby improving the overall experimental accuracy.

Cell Distortion Parameter

The cell-distortion parameter for the volume used in the isochoric experiments ($V_A + V_C$ in Figure 1) was determined from a complete Burnett-isochoric run for pure helium over the ranges $100 \leq T/\text{K} \leq 300$ and $0 \leq P/\text{MPa} \leq 5$. The cell distortions were calculated by an iterative procedure. The uncorrected data first were analyzed using Eqs. 9 and 10 with $\gamma = \gamma' = 0$ to obtain approximate compressibility factors, then trial distortion parameters were calculated using these estimates. After using the trial parameters to correct the raw data, compressibility factors again were obtained, and the procedure was repeated until no further change was observed. A single iteration provided convergence because of the small departures from ideality for helium in this pressure and temperature range. The distortion parameter represented as a function of temperature and base-isotherm pressure by a purely empirical correlation is:

$$\eta = V/V^b = 1 + [a + s(P^b)^q]\,(T - T^b) \qquad (18)$$

Here $a = 5.0 \times 10^{-7}K^{-1}$, $s = 7.04 \times 10^{-6}\,(\text{psia})^{-q}K^{-1}$, and $q = 0.0905$. We note that a represents the thermal expansion of Invar.

Pure-Helium Results

We analyzed the pure-helium data using the pressure virial series because of the high reduced temperatures. Eq. 9 was used to obtain virial coefficients for each experimental temperature. At every temperature, only the second pressure virial coefficient was necessary to provide an adequate fit for our pressure and temperature range. Density virial coefficients then were calculated using:

$$\beta_2 = \beta_2' RT \qquad (19)$$

When the analysis was performed using the individual data or using smoothed polynomial fits to the isochoric data, no sig-

TABLE 1. SECOND VIRIAL COEFFICIENT OF HELIUM

Temp. (K)	B_{He} (cm^3/mol)
100.00	11.3
125.00	11.9
150.00	12.1
175.00	12.12
200.00	12.10
225.00	12.06
250.00	12.02
273.16	11.95
275.00	11.94
300.00	11.81

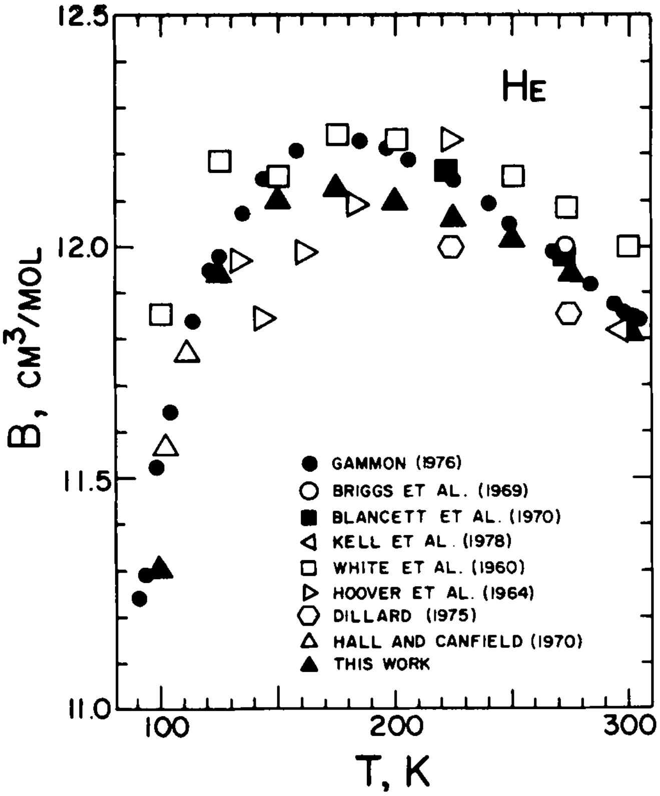

Figure 5. Comparison of results for second virial coefficient of He.

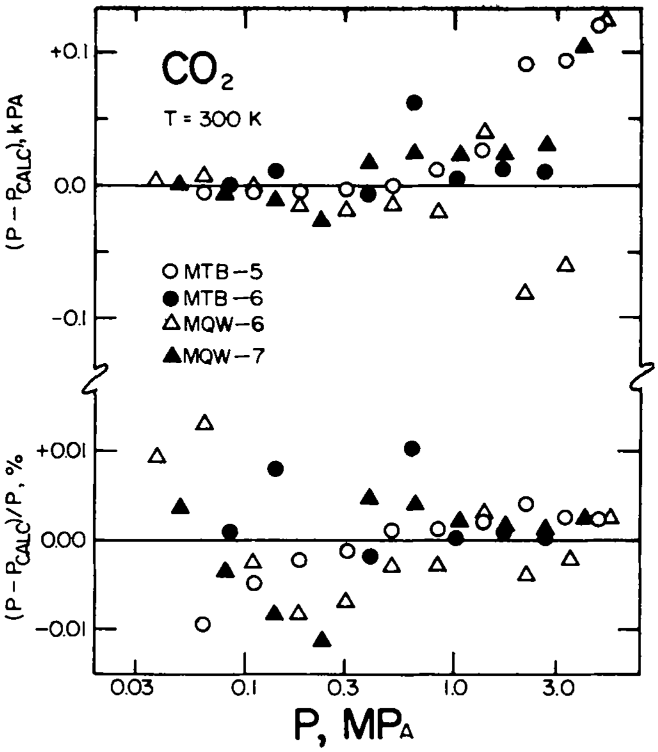

Figure 6. Deviation of CO_2 pressure data from the best fit to all data using Eq. 10 (fit parameters listed in Table 2).

nificant differences appeared. Table 1 contains our pure-helium second virial coefficients, and Figure 5 presents the excellent agreement between our results and those of selected other workers.

The reproducibility of our pure-helium results at 300 K is approximately ±0.1 cm^3/mol, as determined from the numerous experiments required to determine the various apparatus constants and to recalibrate the apparatus after minor repairs. The results of these experiments, as well as all the experimental pressure and temperature data (including the results presented here), are available in Bellomy (1976), Watson (1978), and Young (1978).

The helium sample was certified as 99.9999% pure when received from the U.S. Bureau of Mines. It was, however, used without drying provisions after storage in a steel cylinder for several years. As a result, it may have contained up to 0.02 mol % water. After including realistic estimates for the uncertainties due to sample purity and pressure distortion effects, we feel that the overall uncertainty for our results is better than ±0.3 cm^3/mol. The agreement shown in Figure 5, therefore, is well within the combined experimental errors.

Pure Carbon Dioxide Results

The interaction virial coefficient experiment requires explicit compressibility factor information for the pure fluids only at the mixing temperature. Therefore, we ran CO_2 isotherms only at 300 K. We have accumulated (over several months) a total of four conventional Burnett runs. Two runs were made by each of two different experimenters, and the apparatus was repaired in the interim (with a significant change in apparatus constant). Table 2 reveals the internal consistency of this entire data set, where we

TABLE 2. PURE CARBON DIOXIDE RESULTS (T = 300.00 K)

Data Set	Number Data Points	Second Virial Coefficient (cm^3/mol)	Third Virial Coefficient (cm^6/mol^2)	Apparatus Constant	Minimum Density (mol/m^3)	RMSD Pressure Residual (%)
All Runs:	39	−121.70	4926.7			0.0063
MTB-5				1.677772	26.136	
MTB-6					33.516	
MQW-6				1.685184	19.782	
MQW-7					15.261	
MTB Apparatus:	18	−121.55	4883.2	1.677728		0.0056
MTB-5					26.138	
MTB-6					33.514	
MQW Apparatus:	21	−121.80	4953.1	1.685209		0.0062
MQW-6					19.782	
MQW-7					15.261	
Individual Runs:						
MTB-5	10	−121.65	4914.2	1.677733	26.138	0.0011
MTB-6	8	−121.73	4968.4	1.677773	33.512	0.0048
MQW-6	11	−121.75	4946.0	1.685180	19.783	0.0062
MQW-7	10	−121.84	4962.6	1.685233	15.261	0.0060

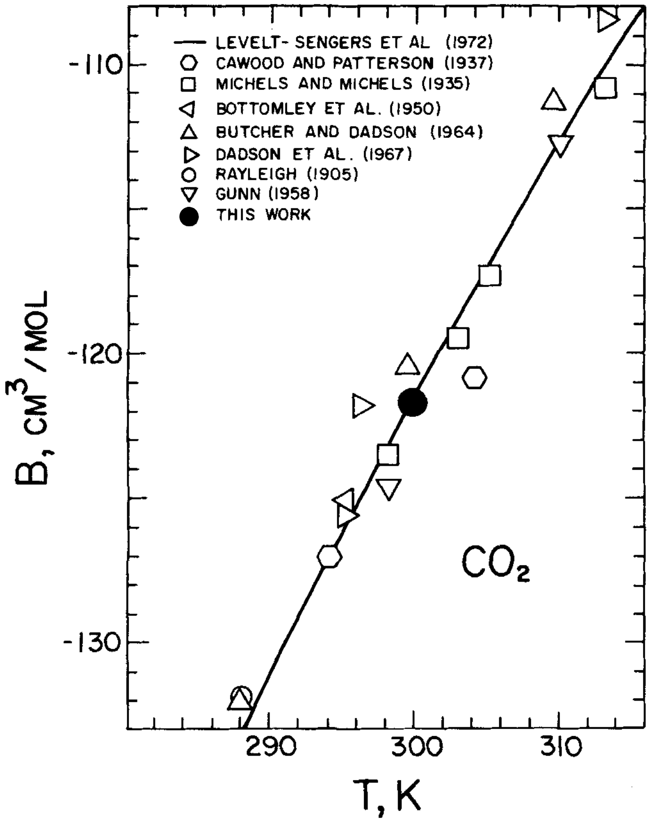

Figure 7. Comparison of results for second virial coefficient of CO_2: size of closed circle, estimated uncertainty; recent experimental data of Waxman et al. are in excellent agreement with correlation of Levelt-Sengers et al.

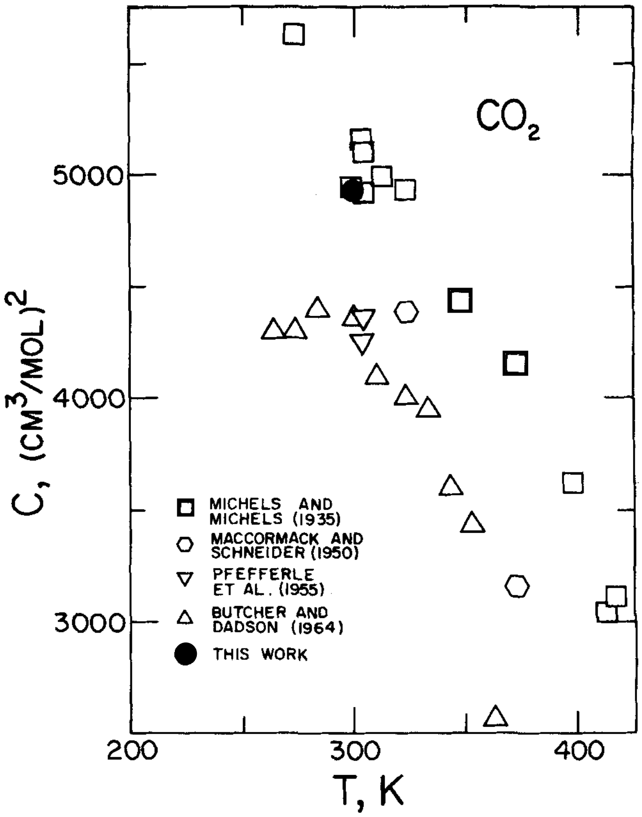

Figure 8. Comparison of results for third virial of CO_2: size of closed circle, reproducibility of our result.

show the results for all data combined, for each individual experimenter, and for each individual run. These results are indicative of the general reproducibility of our measurements. The deviations of the pressure data from the fit of Eq. 12 to all the data appear in Figure 6 as an illustration of the overall precision of the experiment. We note that only eight adjustable parameters in the model fit thirty-nine data points. The density virial equation is necessary for carbon dioxide, because the proximity of the critical temperature would require too many terms in the pressure series and adversely affect evaluation of the virial coefficients.

The CO_2 sample was certified as more than 99.996% pure by the supplier, Precision Gas Products, at the time of purchase. This sample also was not dried upon removal from the cylinder, but the water problem discussed previously should not be important here due to the presence of substantial amounts of liquid carbon dioxide in the cylinder. The reproducibility of our data, coupled with estimates of the possible error contributions due to sample-purity and pressure-distortion effects, leads to an overall uncertainty estimate of ±0.5 cm³/mol for the CO_2 second virial coefficient results. Overall estimates for the uncertainty in third virial values are crude at best, but we note the ±1% reproducibility among our four runs. Our second-virial coefficient results are compared to the other reported values in Figure 7, where the size of the closed circle indicates the overall estimated uncertainty in our results. Figure 8 compares third-virial results; here the size of the closed circle indicates the reproducibility of our data. The agreement with previous workers is excellent for both the second and third virial coefficients for carbon dioxide.

He-CO_2 Interaction Virial

Two series of mixing experiments were performed on the helium-carbon dioxide system. The first consisted of mixing experiments performed at 300 K with no isochoric extension, while the second included isochoric extension to the dew point curve after mixing at 300 K. In the first case, we measured the pressure of each fluid as the appropriate cells were filled. The fluids then were mixed thoroughly, and the mixture pressure recorded. The isochorically extended data were more complicated. The desired filling pressures were selected, then pure-fluid isochores were run, beginning at the pressure chosen for each pure fluid. The appropriate cell volumes then were filled to the chosen pressures, and the fluids mixed. After mixing, an entire mixture isochore was measured. In each case, the experiment was repeated several times to provide an unambiguous extrapolation of B_{12}^* to zero pressure. The experimental pressure and temperature data and the explicit experimental procedures appear in Bellomy (1976) and Watson (1978) for the first and second sets respectively.

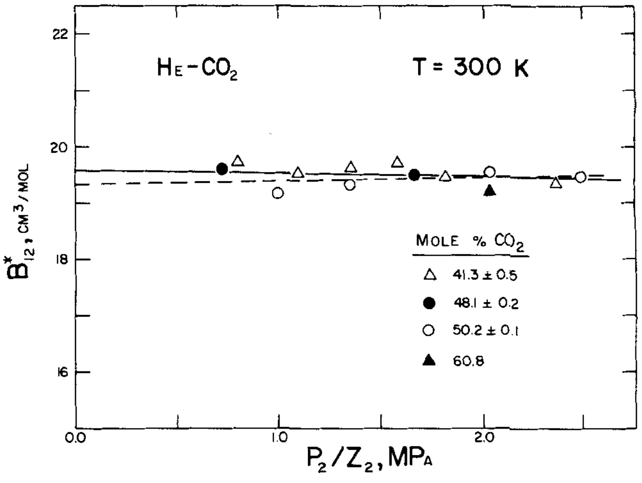

Figure 9. Experimental B_{12} data at 300 K: solid line, best fit of a linear function to all data; dashed line, best fit to all circles. Experimental value of B_{12} is determined from the left-hand intercept. Uncertainties listed with the compositions represent the extreme variation in composition over the entire set of samples with that symbol.

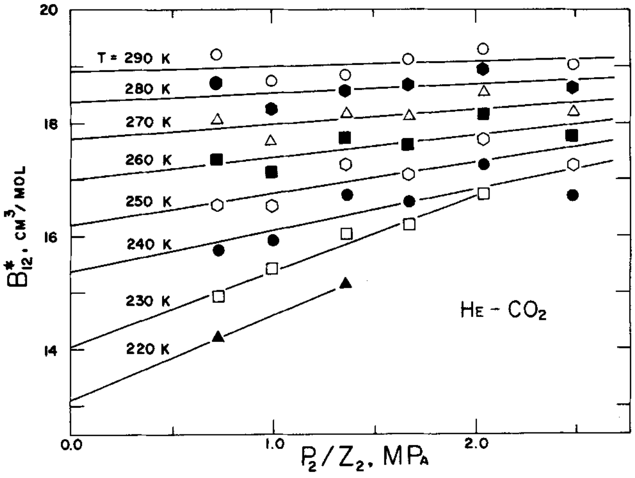

Figure 10. Experimental B_{12} values for isochorically extended mixtures: solid lines, best fit of a linear function to the data for respective isotherms. Experimental value of B_{12} is determined from the left-hand intercept.

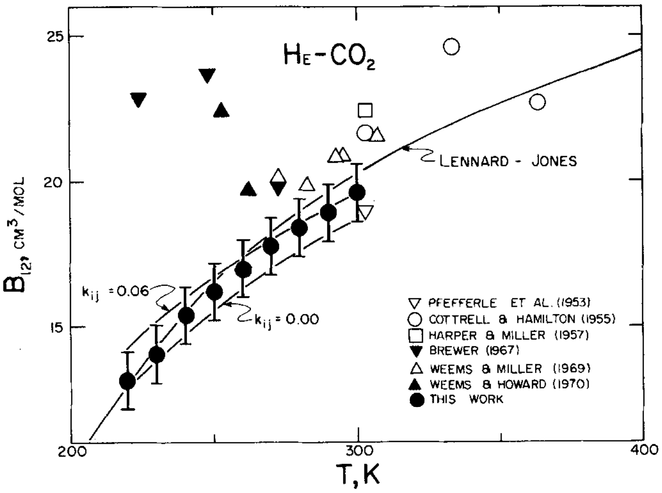

Figure 11. Comparison of B_{12} results. The solid line was calculated using a Lennard-Jones model with simple mixing rules. The curves k_{ij} = 0.00 and 0.06 were calculated using the correlation of Tsonopoulos.

TABLE 3. INTERACTION SECOND VIRIAL COEFFICIENTS FOR HE-CO$_2$ SYSTEM

Temp. (K)	B_{12} (cm^3/mol) Experimental:	Calculated:
220.00	13.1	—
230.00	14.1	14.46
240.00	15.4	15.47
250.00	16.2	16.47
260.00	17.0	17.46
270.00	17.7	18.27
280.00	18.4	18.93
290.00	18.9	19.60
300.00	19.6	20.27

Figure 9 presents the experimental mixing data as a function of P_2/Z_2 for all the 300 K data. These data, acquired on mixtures of four compositions ranging from 40 to 60 mol % CO$_2$, agree within ±0.5 cm^3/mol. The triangles represent the mixing-only data, while the circles represent the isochorically extended mixtures. Strictly speaking, the extrapolation to zero pressure should include only points at constant composition with the same apparatus constants (e.g., open circles or open triangles), but since the differences here are not significantly larger than the experimental imprecision, we have chosen to fit all the points to the same curve. The solid line represents a least-squares fit of a linear function to all the data, while the dashed line represents a fit which includes only the isochorically extended mixtures. The differences are not significant within the precision of the experiment. Third-virial contributions to B^*_{12} are not significant at this temperature, as the slopes are essentially zero.

The isochorically extended data appear in Figure 10, along with the least-squares fit to the data at each temperature. The experimental precision does not change significantly with temperature, but the magnitude of the third-virial contribution does increase substantially as the temperature decreases. The experimental values for the actual interaction second virial coefficient, B_{12}, are the zero-pressure intercepts of the least-squares fits to the data.

The He-CO$_2$ results appear in Table 3, where the 300 K value includes all data in Figure 9. The 300 K value becomes 19.3 cm^3/mol when only the isochorically extended mixtures are used, but the statistical uncertainty overlaps the difference. Systematic errors should not exceed the experimental precision greatly for reasons discussed in the following section. Therefore, based on a 99% *confidence limit*, the uncertainties in our B_{12} values are estimated to be ±1.0 cm^3/mol.

Figure 11 compares our results to those reported by other workers. In general, our values lie below those previously reported, but significant differences exist only with respect to the low-temperature data of Brewer (1967), and Weems and Howard (1970). In both cases, however, their temperature dependence indicates a large experimental uncertainty.

Calculated B_{12} values based on the Lennard-Jones intermolecular potential function also appear in Table 3 and Figure 11. We used the simple combining rules $\epsilon_{12} = \sqrt{\epsilon_{11}\epsilon_{22}}$ and $\sigma_{12} = \frac{1}{2}(\sigma_{11} + \sigma_{22})$, where the pure-component parameters are those selected by Mason and Spurling (1969). Hirschfelder et al. (1954) provide a sample calculation following this procedure. The agreement is remarkable (although probably fortuitous), as the calculated value lies within the estimated experimental uncertainty of our experimental point in every case.

We also have used the modification of the Pitzer and Curl (1957) correlation for second virial coefficients given by Tsonopoulos (1974) to determine a binary interaction parameter, k_{ij} = 0.03 ± 0.03, for the He-CO$_2$ system. We used pure-fluid critical properties from Reid, Prausnitz, and Sherwood (1977) for carbon dioxide and the classical values recommended by Prausnitz (1969) for helium. The curves corresponding to the extreme values of k_{ij} are compared in Figure 11.

Errors in B_{12} Determination

The principal sources of error in the B_{12} determinations are: a) uncompensated higher-order virial effects; b) pressure-distortion effects on the cell volume; c) random pressure-measurement errors; d) errors in the determination of the apparatus constants or the pure-fluid compressibility factors; and e) adsorption effects. We shall now consider the influence of each of these factors on our results, in particular, on the plots of B^*_{12} vs. P_2/Z_2.

The technique for eliminating errors due to higher-order virial contributions has been discussed already (Eq. 17, for example). A truly unambiguous extrapolation of B^*_{12} vs. P_2/Z_2 to zero pressure would eliminate completely the higher-order virial effects, but experimental imprecision always introduces some ambiguity. The primary practical problem encountered here is maintaining a constant composition over an entire series of mixtures. Fortunately, for the CO$_2$-He system, the effect of composition appears to be insignificant.

The distortion of the cell volumes with pressure is the most difficult source of error to analyze and to detect. We have used a computer simulation to determine that the effect on the pure-fluid virial coefficient determinations should be less than 0.1 cm^3/mol. To minimize the effects on the B_{12} experiment, we use apparatus constants and pure-fluid compressibility factors determined for a particular volume with the pure fluid to be used in that volume in the mixing experiment. In this manner, some of the undetected cell-distortion errors should cancel.

Pressure-measurement errors will introduce random scatter into the B^*_{12} vs. P_2/Z_2 plot. Only extreme precision (significantly better than 0.01%) in pressure measurements will provide acceptable precision in B_{12} determinations, because B^*_{12} *involves small differences in large terms.* Pressure measurements of a precision illustrated in Figure 6 will provide precision better than 0.5 cm^3/mol in B^*_{12}. Errors from this source become obvious in the analysis plots (B^*_{12} vs. P_2/Z_2).

Errors in the prior determinations of apparatus constants, cell-distortion parameters, and pure-fluid properties will appear as systematic errors on the analysis plots, because the same determinations will be used throughout the entire series of mixtures. In general, the effect on B_{12} of systematic errors in the variables O_i will be given by:

$$\delta B_{12} = \sum_i \frac{\partial B_{12}}{\partial O_1} O_i \qquad (20)$$

A careful consideration of Eq. 16 shows that:

$$\frac{\partial B^*_{12}}{\partial O_i} = K_i\left(\frac{Z_2}{P_2}\right)^u \quad (u = 1 \text{ or } 2) \qquad (21)$$

where K_i is essentially constant. Then, any significant systematic error in the N_i, Z_i, or η_i must appear as curvature, $(P_2/Z_2)^{-1}$ or $(P_2/Z_2)^{-2}$, on the analysis plot. The precision of the B^*_{12} values then becomes the limiting factor for the detection of systematic errors, and such errors cannot greatly exceed the experimental precision. We do note that an error in Z that is linearly or quadratically proportional to the pressure would be difficult to detect.

Errors due to adsorption effects are difficult to detect and describe quantitatively. Such effects are pressure-dependent, however, and they tend to zero as the pressure approaches zero. As a result, an unambiguous extrapolation of the analysis plot to zero pressure tends to minimize or eliminate any possible adsorption effects as well.

The accuracy of determination of the interaction second virial coefficient then depends principally on an accurate extrapolation of the plot of B^*_{12} vs. P_2/Z_2 to zero pressure. Most significant sources of error introduce either random scatter or curvature in this plot. Therefore, the uncertainty in the experimental determination of B_{12} cannot greatly exceed the uncertainty in the determination of the intercept as P_2/Z_2 (or equivalently, the density) goes to zero. Appropriate analysis of the experimental data, therefore, provides a powerful test for the presence of significant random or systematic errors.

ACKNOWLEDGMENTS

The authors gratefully acknowledge financial support for this work from the following sources: NSF Grants ENG 77-01070 and ENG 76-00692, GPA Project 772, AGA Grant BR 110-2, and GRI Grant 5014-363-0118. Acknowledgment is made to the donors of the Petroleum Research Fund, administered by the American Chemical Society, for partial support of this research. The assistance of Dr. Patrick J. White in the preparation of many of the computer programs used in this work is also gratefully noted.

Appendix A

The virial equation of state for a fluid (either mixture or pure) may be expressed as:

$$P_i = \rho_i Z_i RT = RT \sum_{k=1}^{\infty} \beta_k \rho_i^k \quad (i = 1, 2, m) \qquad (A1)$$

We now insert an interaction model into Eq. A1 to determine interaction second virial coefficients from data for binary mixtures. For such binaries, Eqs. 2 and 3 become:

$$\beta_{2m} = B_m = y_1^2 B_{11} + 2y_1y_2B_{12} + y_2^2B_{22} \qquad (A2)$$

and

$$\beta_{3m} = C_m = y_1^3C_{111} + 3y_1^2y_2C_{112} + 3y_1y_2^2C_{122} + y_2^3C_{222} \qquad (A3)$$

Here, subscripts 1 and 2 denote the properties of the respective pure fluids and m denotes mixture properties. The apparatus constants can be expressed by an alternative relationship as:

$$N_i = \rho_i/\xi_i \quad (i = 1, 2) \qquad (A4)$$

where ρ_i is the density of pure fluid i *before mixing*, and ξ_i is the density of component i *in the mixture.* We note that this ratio is equal to the ratio of the final mixture volume to the original volume of the pure fluid i, or equivalently, to the cell constant for an expansion of i from its original volume into the volume containing the mixture. The composition and the total mixture density are:

$$y_i = \xi_i/\rho_m \qquad (A5)$$

and

$$\rho_m = \xi_1 + \xi_2 \qquad (A6)$$

Eqs. A2, A3, and A5 lead to:

$$\rho_m^2 B_m = \xi_1^2 B_{11} + 2\xi_1\xi_2B_{12} + \xi_2^2B_{22} \qquad (A7)$$

and

$$\rho_m^3 C_m = \xi_1^3C_{111} + 3\xi_1^2\xi_2C_{112} + 3\xi_1\xi_2^2C_{122} + \xi_2^3C_{222} \qquad (A8)$$

Substitution of Eqs. A7 and A8 into Eq. A1 yields:

$$P_m = RT(\xi_1 + \xi_2 + \xi_1^2B_{11} + 2\xi_1\xi_2B_{12} + \xi_2^2B_{22} + \rho_m^3C_m + \ldots) \qquad (A9)$$

The terms containing the pure-fluid virial coefficients B_{11} and B_{22} now can be eliminated using the equations of state for the pure fluids. We note that:

$$P_i/N_i^2 = \xi_i/N_i + \xi_i^2B_{ii} + N_i\xi_i^3C_{iii} + \ldots \quad (i = 1, 2) \qquad (A10)$$

Then,

$$P_m - P_1/N_1^2 - P_2/N_2^2 = RT[\xi_1(1 - 1/N_1) + \xi_2(1 - 1/N_2) + 2\xi_1\xi_2B_{12} + \Phi_3 + \ldots] \qquad (A11)$$

where the contribution due to third virial effects, Φ_3, is:

$$\Phi_3 = (1 - N_1)\xi_1^3C_{111} + 3\xi_1^2\xi_2C_{112} + 3\xi_1\xi_2^2C_{122} + (1 - N_2)\xi_2^3C_{222} \qquad (A12)$$

The entire result can now be expressed in terms of pure fluid properties, apparatus constants, and the pressure data by using the relationship:

$$\xi_i = \rho_i/N_i = P_i/N_iZ_iRT \quad (i = 1, 2) \qquad (A13)$$

Eq. A11 then becomes:

$$\frac{N_1N_2Z_1Z_2RT}{2P_1P_2}\left[P_m - \frac{P_1}{Z_1N_1^2}(N_1 + Z_1 - 1) - \frac{P_2}{Z_2N_2^2}(N_2 + Z_2 - 1)\right] = B_{12} + \frac{N_1N_2}{2\rho_1\rho_2}\Phi_3 + \ldots \qquad (A14)$$

In this expression, all quantities in the left-hand expression represent experimental observables which are measured either during the Burnett-mixing experiment or during previous experiments on the individual pure fluids. The leading term on the right is the property of interest and the second term is directly related to third virial coefficient effects. We now examine the third virial term in detail. Combination of Eqs. A12 and A13 leads to:

$$\frac{N_1N_2}{2\rho_1\rho_2}\Phi_3 = \frac{1}{2}\xi_2X^{-1}[(1 - N_1)C_{111}X^3 + 3C_{112}X^2 + 3C_{122}X + (1 - N_2)C_{222}] = \frac{P_2}{Z_2}\left[\frac{1}{2RTN_2}f(X)\right] \qquad (A15)$$

where

$$X = \xi_1/\xi_2 = y_1/y_2 = y_1/(1 - y_1) \tag{A16}$$

Then, for a series of mixing experiments performed at constant composition (X), the third-virial contribution varies linearly with P_2/Z_2. Similar arguments applied to the higher-order contributions lead to the conclusion that:

$$B_{12} + \frac{N_1N_2}{2\rho_1\rho_2}\Phi_3 + \ldots = B_{12} + A_1(P_2/Z_2) + A_2(P_2/Z_2)^2 + \ldots \tag{A17}$$

where the A_k are constant for constant composition. The left-hand side of Eq. A17 is what we observe experimentally and we label it:

$$B_{12}^* = B_{12} + \frac{N_1N_2}{2\rho_1\rho_2}\Phi_3 + \ldots \tag{A18}$$

For the isochorically extended experiment, Eqs. A11 and A12 become respectively:

$$\eta_m^2P_m - \frac{\eta_1^2P_1}{N_1^2} - \frac{\eta_2^2P_2}{N_2^2} = RT[\xi_1^b(\eta_m - \eta_1/N_1) + \xi_2^b(\eta_m - \eta_2/N_2) + 2\xi_1^b\xi_2^bB_{12} + \Phi_3 + \ldots] \tag{A19}$$

$$\Phi_3(T) = \left(\frac{1}{\eta_m} - \frac{N_1}{\eta_1}\right)\xi_1^{b^3}C_{111} + \frac{3}{\eta_m}\xi_1^{b^2}\xi_2^bC_{112} + \frac{3}{\eta_m}\xi_1^b\xi_2^{b^2}C_{122} + \left(\frac{1}{\eta_m} - \frac{N_2}{\eta_2}\right)\xi_2^{b^3}C_{222} \tag{A20}$$

These expressions lead to Eqs. 16 and 17 in the body of the paper.

NOTATION

a = constant
A_i = constant
B = second virial coefficient
B' = second virial coefficient for pressure-explicit form of virial equation
B_{ij} = interaction second virial coefficient
B_{ij}^* = uncorrected observed interaction second virial coefficient
C = third virial coefficient
C' = third virial coefficient for pressure form of virial equation
C_{ijk} = interaction third virial coefficient
k_{ij} = binary interaction parameter
K_i = constant
N = apparatus constant
O_i = observable
P = pressure
q = exponent
R = gas constant
s = constant
T = temperature
u = exponent
V = volume
X = ratio of mole fractions
y_i = mol fraction of component i in vapor phase
Z = compressibility factor

Greek Letters

β_k = general virial coefficient
γ = pressure-distortion coefficient
δ = error operator
ϵ = Lennard-Jones energy parameter
η = cell-distortion parameter
ξ_i = density of component i in the mixture
ρ = density
σ = Lennard-Jones separation parameter
Φ = third virial contribution to B_{12}^*

Subscripts

A,B,C = various volumes in a Burnett cell
i = component i
j = component j or expansion number
k = index
m = mixture

Superscripts

b = base isotherm or mixing temperature property
$'$ = property after Burnett expansion is made; also denotes virial coefficients in pressure-explicit virial equation

LITERATURE CITED

Angus, S., B. Armstrong, and K. M. de Reuck, ed., *International Thermodynamic Tables of the Fluid State: Carbon Dioxide*, Pergamon Press, Oxford (1973).

Angus, S., and K. M. de Reuck, ed., *International Thermodynamic Tables of the Fluid State: Helium-4*, Pergamon Press, Oxford (1975).

Bammert, V. K., and R. Klein, "Das reale Verhalten der Gasmischungen Helium-Neon, Helium-Stickstoff und Helium-Kohlendioxide im Bereich von 0 bis 1000°C und 1 bis 100 bar," *Atomikernenergie*, Bd. 24, Lfg. 3 (1974).

Barieau, R. E., "Helium-4 Experimental P-V-T," U.S. Dept. of Interior, Info. Circular No. 8388 (1968).

Bellomy, M. T., "An Experimental Verification of the Hall and Eubank Method of Direct Measurement of the Interaction Second Virial Coefficient," M.S. Thesis, Texas A&M University, College Station, TX (1976).

Blancett, A. L., K. R. Hall, and F. B. Canfield, "Isotherms for the He-Ar System at 50°C, 0°C and −50°C up to 700 atm," *Physica*, **47**, 75 (1970).

Bottomly, G. A., D. S. Massie, and R. Whytlaw-Gray, "A Comparison of the Compressibilities of Some Gases with That of Nitrogen at Pressures Below 1 Atmosphere," *Proc. Roy. Soc. London*, **A200**, 201 (1950).

Brewer, J., "Determination of Mixed Virial Coefficients," Midwest Research Inst., Kansas City, MO, Rept. No. MRL-2915-C, AFOSR-67-2795 (1967).

Briggs, T. C., B. J. Dalton, and R. E. Barieau, "Compressibility Data for Helium at 0°C and Pressures to 800 Atmospheres," *U.S. Bur. Mines Rept. Inv.*, **7287** (1969).

Britt, H. I., and R. H. Luecke, "The Estimation of Parameters in Nonlinear, Implicit Models," *Technometrics*, **15**, No. 2, 233 (1973).

Burnett, E. S., "Compressibility Determinations Without Volume Measurements," *Appl. Mech.*, **3**, No. 4, A136 (1936).

Burnett, E. S., "Application of the Burnett Method of Compressibility Determinations to Multiphase Fluid Mixtures," *U.S. Bur. Mines Rept. Inv.*, **6267** (1963).

Butcher, E. G., and R. S. Dadson, "The Virial Coefficients of the Carbon Dioxide-Ethylene System," *Pro. Roy. Soc. London*, **A277**, 448 (1964).

Cawood, W., and H. S. Patterson, "The Determination of Atomic Weights by Means of the Microbalance, and the Values Obtained for Carbon, Nitrogen, and Fluorine," *Phil. Trans. Roy. Soc. London*, **A236**, 77 (1937).

Cook, G. A., ed., *Argon, Helium and the Rare Gases*, **I**, Interscience Publishers, New York (1961).

Cottrell, T. L., and R. A. Hamilton, "The Second Virial Coefficient of Gases and Mixtures," *Trans. Far. Soc.*, **52**, 156 (1956).

Dadson, R. S., E. J. Evans, and J. H. King, "The Second Virial Coefficient of Carbon Dioxide," *Proc. Phys. Soc., London*, **92**, 115 (1967).

Dillard, D. D., M. Waxman, and R. R. Robinson, "Volumetric Properties of the He-Kr System at Moderate T&P," *J. Chem. Engr. Data*, **23**, 269 (1978).

Dymond, J. H., and E. B. Smith, *The Virial Coefficients of Gases: A Critical Compilation*, Clarendon Press, Oxford (1969).

Edwards, A. E., and H. E. Roseveare, "The Second Virial Coefficients of Gaseous Mixtures," *J. Chem. Soc.*, **64**, 2816 (1942).

Gammon, B. E., "The Velocity of Sound With Derived State Properties in Helium at −175 to 150°C With Pressure to 150 atm," *J. Chem. Phys.*, 4, 2556 (1976).

Gunn, R. D., "Volumetric Properties of Non-Polar Gas Mixtures," M.S. Thesis, Univ. of California, Berkeley, CA (1958).

Hall, K. R., and F. B. Canfield, "Optimal Recovery of Virial Coefficients from Experimental Compressibility Data," *Physica*, **33**, 481 (1967).

Hall, K. R., and F. B. Canfield, "Isotherms for the He-N_2 System at −190°C, −170°C and −160°C up to 700 atm," *Physica*, **47**, 219 (1970).

Hall, K. R., and P. T. Eubank, "Burnett-Isochoric Coupled Data with Application to Adsorbing Gases," *Physica*, **61**, 346 (1972).

Hall, K. R., and P. T. Eubank, "Experimental Technique for Direct Measurement of Interaction Second Virial Coefficients," *J. Chem. Phys.*, **59**, 709 (1973).

Hall, K. R., and P. T. Eubank, "Mixture Compositions and Excess Volumes from the Burnett Apparatus," *AIChE J.*, **20**, 815 (1974).

Hall, K. R., and W. Righter, "Optimal Truncation of the Virial Equation," *AIChE J.*, **21**, 406 (1975).

Harper, Jr., R. C., and J. G. Miller, "Compressibility of Gases II. Mixtures of Carbon Dioxide and Helium at 30°C," *J. Chem. Phys.*, **27**, No. 1, 36 (1957).

Hirschfelder, J. O., C. F. Curtiss, and R. B. Bird, "Molecular Theory of Gases and Liquids," 170, John Wiley and Sons, Inc., New York (1954).

Holste, J. C., P. T. Eubank, and K. R. Hall, "Optimum Use of a Differential Pressure Transducer for High-Precision Measurements," *Ind. Eng. Chem., Fund.*, **16**, 378 (1977).

Hoover, A. E., F. B. Canfield, R. Kobayashi, and T. W. Leland, "Determination of Virial Coefficients by the Burnett Method," *J. Chem. Eng. Data*, **9**, No. 4, 568 (1964).

Kell, G. S., G. E. McLaurin, and E. Whalley, "Second Virial Coefficient of Helium from 0 to 500°C by the Two Temperature Expansion Method," *J. Chem. Phys.*, **68**, 2199 (1978).

Knobler, W. H., J. J. M. Beenakker, and H. F. P. Knapp, "The Second Virial Coefficient of Gaseous Mixtures at 90°K," *Physica*, 25 909 (1959).

Kuenen, J. P., and W. W. Randall, "The Expansion of Argon and Helium as Compared with that of Air and Hydrogen," *Proc. Roy. Soc. London*, **59**, 60 (1895).

Lee, S. M., P. T. Eubank, and K. R. Hall, "Truncation Errors Associated with the Virial Equation," *J. Fluid Phase Eq.*, **1**, 219 (1978). [Corrigendum for Figure 1: **2**, 315 (1979)].

Levelt-Sengers, J. M. H., M. Klein, and J. S. Gallagher, "Pressure-Volume-Temperature Relationships of Gases; Virial Coefficients," *American Institute of Physics Handbook*, 3rd ed., ed., D. E. Gray, McGraw-Hill Book Co., New York (1972).

Linshits, L. R., I. B. Rodkina, and D. S. Tsiklis, "Measurement of the Compressibilities of CO_2-He Mixtures by Burnett's Method," *Zhur. Fiz. Khim.*, **49**, 2141 (1975).

Mansoorian, H., E. F. Capps, H. L. Gielen, P. T. Eubank, and K. R. Hall, "Compact, Magnetic Recirculating Pump for Wide Range Temperature and Pressure Operation," *Rev. Sci. Instrum.*, *46*, No. 10, 1350 (1975).

Mason, E. A. and T. H. Spurling, "The Virial Equation of State," 269, Pergamon Press, Oxford (1969).

McCormack, K. E., and W. G. Schneider, "Compressibility of Gases at High Temperatures, IV. Carbon Dioxide in the Temperature Range 0°-600°, and Pressures up to 50 Atmospheres," *J. Chem. Phys.*, 18, No. 9, 1269 (1950).

Michels, A., and C. Michels, "Isotherms of CO_2 between 0° and 150° and Pressures from 16 to 250 Atm (Amagat Densities 18-206)," *Proc. Roy. Soc. London*, **A153**, 201 (1935).

Pak, N., and S. Schultz, "Determination of Mixing Effects in a CO_2-He Gas Mixture with a Modified Burnett Apparatus," *Chem. Ing. Tech.*, **50**, No. 11, 889 (1978).

Pfefferle, Jr., W. C., J. A. Goff, and J. G. Miller, "Compressibility of Gases I. The Burnett Method. An Improved Method of Treatment of the Data. Extension of the Method to Gas Mixtures," *J. Chem. Phys.*, **23**, No. 3, 509 (1955).

Pitzer, K. S., and R. F. Curl, Jr., "Empirical Equation for the Second Virial Coefficient," *J. Amer. Chem. Soc.*, **79**, 2369 (1957).

Pope, G. A., P. Chappelear, and R. Kobayashi, "Analysis of Data Obtained by Isochorically Coupled Burnett Experiments," *Physica*, **57**, 127 (1972).

Prausnitz, J. M., *Molecular Thermodynamics of Fluid-Phase Equilibria*, Englewood Cliffs, NJ (1969).

Rayleigh, L., "IX. On the Compressibility of Gases Between One Atmosphere and Half an Atmosphere of Pressure," *Philos. Trans. Roy. Soc. London*, **A204**, 351 (1905).

Reid, R. C., J. M. Prausnitz, and T. K. Sherwood, *The Properties of Gases and Liquids*, 3rd ed., McGraw-Hill, N.J. (1977).

Tsonopoulos, C., "An Empirical Correlation of Second Virial Coefficients," *AIChE J.*, **20**, 263 (1974).

Vennix, A. J., "Low Temperature Volumetric Properties and Development of an Equation of State for Methane," Ph.D. Dissertation, Rice Univ., Houston, TX (1965).

Vukalovich, M. P., and V. V. Altunin, *Thermophysical Properties of Carbon Dioxide*, Collet's Ltd., London (1968).

Watson, M. Q., "The Interaction Second Virial Coefficient for the He-CO_2 System between 230 and 300 K," M.S. Thesis, Texas A&M Univ., College Station, TX (1978).

Waxman, M., H. A. Davis, and J. R. Hastings, "A New Determination of the Second Virial Coefficient of Carbon Dioxide at Temperatures between 0° and 150°C and an Evaluation of its Reliability," *6th Symp. Thermophys. Prop.*, Atlanta (1973).

Weber, L. A., "Thermodynamic and Related Properties of O_2 from the Triple Point to 300 K at Pressures to 330 atm," *NBS Rept.*, **9710** (1968).

Weems, G. W., and M. L. Miller, "Compressibility Factors for Helium and Carbon Dioxide Mixtures at 0 Degrees, 10 Degrees, 20 Degrees, 23 Degrees and 35 Degrees C and up to 900 psia," *U.S. Bur. Mines Rept. Inv.*, **7233** (1969).

Weems, G. W., and A. R. Howard, "Compressibility Factors for Helium and Carbon Dioxide Mixtures at −10 Degrees and −20 Degrees C and Pressures to 1,000 psia," *U.S. Bur. Mine Rept. Inv.*, **7412** (1970).

White, D., T. Rubin, P. Camky, and H. L. Johnston, "The Virial Coefficients of Helium from 20 to 300 Degrees K," *J. Phys. Chem.*, **64**, No. 11, 1607 (1960).

Young, J. G., "Interaction Second Virial Coefficients for C_2H_6-CO_2 System between 250 and 300 K," M.S. Thesis, Texas A&M Univ., College Station, TX (1978).

Manuscript received October 12, 1979; revision received April 4 and accepted May 13, 1980.

Modeling Pulverized Coal Conversion in Entrained Flows

A detailed description of pulverized coal conversion in one-dimensional entrained flows has been formulated and correlated to hydrogasification data from the Rockwell International Flash Hydropyrolysis (FHP) reactor using bituminous coals. This analysis contains physical and chemical descriptions which have not been included in previous mathematical models. These descriptions provide further important insights into the nature of entrained flow coal gasification.

K. M. SPROUSE

Energy Systems Group
Rockwell International
Canoga Park, CA 91304

SCOPE

Entrained flow reactors are increasingly becoming an important concept in the processing of coal into synthetic fuels and thermal energy for power generation. This is primarily due to the fact that entrained flow reactor concepts generally produce faster coal gasification rates (through increased coal-gas surface areas which reduce diffusional resistances) and have a greater ease of operability than fluidized or fixed bed reactors operating at the same coal-firing rates.

0001-1541-80-2560-0964-$01.15.